Geosynthetics, J. Kuwano & J. Koseki (eds)

Response of a submerged geocontainer to an underwater explosion shock wave

Tyagi, V.K.
Asian Region, Kolon International Corporation, B-407, Yamunotri, Jangid Complex, Mira Road, Thane -401107 Maharastra, India, vipkolon@yahoo.com

Keywords: geocontainers, shock loading, underwater explosion, structure-acoustic interaction, geotextile

ABSTRACT: The objective of this study was to evaluate the behavior and integrity of the geocontainer under underwater explosion loading conditions. This study will help in selection of proper geosynthetic for fabricating geocontainers, selection of suitable anchoring or strapping system for maintaining stability of geocontainer system. An underwater explosion may be triggered by several reasons like mining operation, sudden landslides or earth quake, bomb explosion, tsunami generation etc. This can be a potential hazard to the safety of the marine structure. This study will help in better designing of geosystem with adequate factor of safeties. A study was initiated to examine the structural response of submerged geocontainer subjected to additional loading due to acoustic pressure shock wave caused by an underwater explosion. This class of problem is characterized by a close interaction between the geocontainer kinematics and the pressures of shock waves on the interfacial surface between the surrounding fluid and the structure. The specific characteristic of this shock loading is the attainment of maximum pressure in very short time by the steep wave front of spherical pressure wave. The pressure decreases exponentially over a significantly longer period of time. Thus, a large frequency range (low, intermediate and high response frequencies) is exhibited by the geocontainer due to underwater explosion shock loading.

1 INTRODUCTION

Geosystems likes geocontainers are basically flexible structures made from geosynthetics for accurate, large scale underwater fill placement and containment; to protect pipelines; to form breakwaters, revetment, groins; to provide support against sliding, and underwater bank protection. They offer the potential for construction of low cost and technically superior alternative solutions out of readily available materials like contaminated dredged fill, industrial or municipal waste material compared to conventional marine structures made of stones, mass concrete, tetrapodes etc.

2 SCOPE OF STUDY

A pilot scale experimental study was conducted in which a geocontainer is placed in submergence and exposed to pressure shock wave produced by an explosive charge. The strain gauge experiment data are filtered to produce strain history curves. The pressure transducers were placed to record the time history curve of incident pressure wave. The numerical modeling was done for simulation of geocontainer behavior under water explosion shock loading. The results obtained from numerically modeling were in close agreement with experimental results and provide a conservative estimate of the geocontainer's peak response and is, therefore, appropriate for meeting the analysis objective.

3 BRIEF REVIEW

Klusman, Plaut, and Suherman have modeled a slurry-filled (modeled as a hydrostatic pressure) geotextile tube supported by a Winkler foundation (Klusman 1998, Plaut and Klusman 1999, and Plaut and Suherman 1998). The results of these include the tube height, ground deflection, membrane tension, and various tube shapes. Suherman and Plaut studied a single tube resting on a Winkler foundation with and without impounding external water. Plaut and Klusman (1999) analyzed single, two stacked, and 2-1 tube configurations resting on a modified Winkler foundation. Huong (2001) and Kim (2003) used the finite difference software of FLAC to model water-filled tubes supported by a Mohr-Coulomb soil

foundation. Dynamic vibrations about the equilibrium configuration were later introduced (Cotton and Plaut 2003).

4 PROBLEM DEFINITION

The prediction of transmit response of submerged geocontainer that experience loading by acoustic pressure shock wave can be used for proper designing for sustaining these type of loads. For the acoustic-structural system where the fluid and structure are both modeled and coupled, the incident wave loading must be defined to act upon both the fluid and structural surfaces at the wetted interface. Acoustic volumetric acceleration loads corresponding to the incident wave are then applied to the fluid surface, while the incident wave pressures are applied to the structural surface. The experimental-analytical correlation at an early time (peak strain prediction) is very good, and also for the dominant response frequency of the geocontainer. The predicted strains oscillation for longer times suggest that modeling of hydrodynamic drag damping and viscous losses by applying mass damping to geocontainer could be improved.

5 EXPERIMENTAL SETUP

The experimental setup consists of submerged geocontainer exposed to pressure shock wave produced by a 25 kg HBX-1 explosive charge as shown in Figure 1. This setup is similar to the experiment conducted by Kwon and Fox (1993), for underwater shock response of a cylinder subjected to a side-on explosion. The test geocontainer is made up of woven polypropylene (PP) geotextile, whose properties are given in Table 1. The concrete slurry was pumped into the geocontainer. It has an overall length of 10 meter, an outside circumference of 3.14 meter, a wall thickness of 5 mm and closed at end by seamed end caps. The geocontainer is placed horizontally in a 50 meter deep test pit filled with marine water. The explosive charge and geocontainer are both placed at a depth of 4 m, with the help of polymeric straps. Normally, the geocontainer is placed on the subgrade. However, it has been placed at this depth to simulate the perfectly symmetric dynamic loading situation, where hydrodynamic forces are significantly larger than the hydrostatic force and subgrade reaction. The charge is centered off the side of geocontainer and is located 8 meter away from the cylinder surface. The suspension depths, charge offset, and the test duration are selected such that cavitations of the fluid are not significant and no bubble pulse occurs. Strain gauges were placed at several locations on the outer surface of the geocontainer, as shown in Figure 1. The strain gauge experimental data are filtered at 2000 Hz by digitizing the strain history curves. Two pressure transducers were positioned 8 meter from the charge, away from the geocontainer but at the same depth as the cylinder. These transducers provide an experimental determination for the pressure verses time history of the spherical incident shock wave as it travels by the point of geocontainer closest to the charge (strain gauge location B_1).

Table 1. Properties of woven geotextile used for fabricating geocontainer.

Geotextile Property	Value
Tensile strength	320 kN/m
Elongation	10%
Seaming strength	320 kN/m
Permeability	0.01 cm/sec
Unit weight	1000 gsm

6 NUMERICAL MODELING

The total acoustic pressure within the fluid consists of an incident wave and a scattered component as the acoustic field behavior will be linear due to absence of cavitations. The shock wave produced by the underwater explosion charge is termed as incident wave. The interaction of the incident wave with the submerged geocontainer gives rise to scattered wave. The nature of incident wave can be determined from either empirical formula or experimental data. In this case, the nature of incident wave is found to be spherical. A spherical incident shock wave is applied as the input load active in both the acoustic and structural meshes at their common surface (the wetted interface), and the external fluid pressure degrees of freedom represent only the unknown scattered component of the total acoustic pressure.

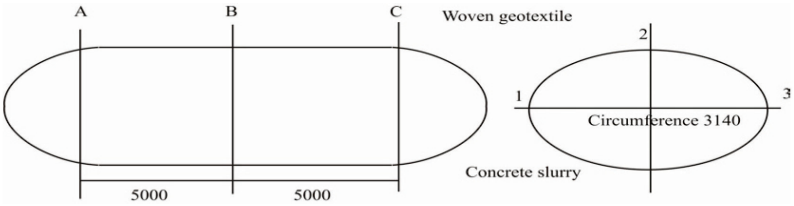

Figure 1. Strain gauge locations at various positions over the geocontainer (in mm).

The finite element shell mesh used for representing the geocontainer has been assumed using finite element software Abaqus 6.5-1. The finite element (S4R) is linear, finite membrane strain, reduced integration, quadrilateral shell element. The element connectivity is such that each shell normal is directed into the external fluid. The nodes are positioned on the out side surface of the geocontainer. The S4R elements adjacent to the end cap are dummy elements with reduced mass and stiffness used only to provide surface that correspond to the thickness of the end caps. Beam type multipoint constraints (MPC_s) are used to tie the end caps (simulation of seaming) to the main geocontainer body. The local 1-direction is aligned with the geocontainer's axis for the main body and is radially directed for the end caps. The local 2-direction is in the circumferential (hoop) direction for both the geocontainer and the end caps.

The finite element selected for meshing the external fluid is 4 noded AC3D4 acoustic tetrahedral elements. The outer boundary of the external fluid is represented by a cylindrical surface with spherical ends. The characteristic radius of the outer boundary is assumed to be 3 meter. The reason for keeping outer boundary at wider distance of 3 meter is to have adequate representation of the added mass associated with the low frequency beam bending modes of the geocontainer. The beam bending mode correspond to an N = 1 sinusoidal translation of the geocontainer's cross-section through the fluid. The added mass effects can be evaluated by assuming the outer boundary of the fluid as rigid (non-radiating) for evaluating the added mass effects when using a plane wave radiation impedance boundary for the external fluid. An appropriate characteristic radius for the external fluid can be determined by deriving an analytical solution for the added mass associated with the translation of an infinite cylinder of radius, R_1, located within a fluid filled infinite cylinder of radius, R_0. The results for analytical solution (Blevins 1979) are shown in Table 2. The characteristic radius is based upon an outer boundary (R_0) to geocontainer radius (R_i) ratio of 6.0, which corresponds to an added mass error of about 6% for infinite cylinders. The outer fluid boundary location can be placed at about half of the distance required when using the plane wave radiation model. The acoustic radiation for the low frequency beam bending modes may not account for the damping caused by hydrodynamic drag and/or fluid viscosity. Therefore, mass proportional damping applied to the geocontainer is used to approximate these types of losses.

Figure 2 shows the mesh generated for the combined configuration of external fluid and geocontainer. The model seeding on the fluid boundary is set at 0.10 m at a response frequency of 1500 Hz. The model seeding on the fluid wetted interface with the geocontainer is set at 0.05 m. at 1500 Hz. The

Table 2. Added mass for N = 1 translation mode of an infinite mode of an infinite geocontainer (fluid between concentric cylinder).

Geocontainer circumference ratio (R0/R1)	Added mass ratio (external boundary/infinite domain)
1.50	2.00
2.00	1.667
4.00	1.133
6.00	1.057
8.00	1.032
16.00	1.008
24.00	1.004

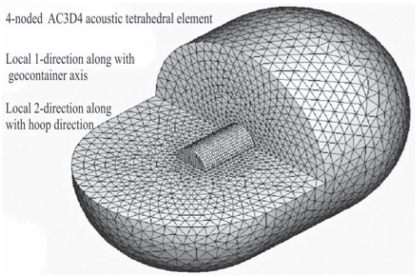

Figure 2. External fluid surface mesh at geotube-acoustic wetted interface.

surface mesh at the acoustic–geocontainer wetted interface is associated with the external fluid. The acoustic mesh being coarser than the structural mesh, the surface of the external fluid at the wetted interface is designated as the master surface. This planning creates an internal coupling of the acoustic pressure and structural displacement of the geocontainer (slave) surface node and ties the geocontainer's acoustic pressure to the fluid mesh acoustic pressure at the wetted interface. For the acoustic-structural system where the fluid and structure are both modeled and coupled, the incident wave loading is defined to act upon both the fluid and structural surfaces at the wetted interface. Acoustic volumetric acceleration loads corresponding to the incident wave are then applied to the fluid surface discussed earlier, while the incident wave pressures are being applied to the geocontainer surface. The finite element selected shown in Figure 2 is not shown with notations as it is a general element which can be universally applied without any specific constraints or limitations. This type of model can be successfully used in similar type of fluid structure interaction problems involving shock loadings of different types.

7 RESULTS AND DISCUSSION

The time history of axial displacement (U_3) for the center nodes of end caps of geocontainer distinctly

show the periodic response associated with a dominant axially directed mode of the geocontainer end cap structure. The 1-direction translation (U_1) of the end cap center nodes is also the primary direction of the shock wave propagation. The response curve obtained illustrates the rigid body translation of the geocontainer, and the oscillations are representative of the fundamental beam-bending mode of the geocontainer. The time history curve of the vertical (U_2) displacement for the nodes location at the top bottom mid plane of the geocontainer suggest that a dominant N = 2 ovalization mode of vibration occurs at about 150 Hz (based on an estimated period of 0.007 seconds). The frequency for the first ovalization mode of the geocontainer in a vacuum is 300 Hz, based upon eigenvalue extraction analysis. This shift in the N = 2 response mode frequency illustrates the added mass effect of the external fluid on the response of the submerged geocontainer.

The time history of the geocontainer strains were obtained from the analysis with experimental data for locations B_1, C_1 and A_2. The experimental curves are obtained by digitizing the response plots published by Kwon and Fox (1993). The digitized curves are shifted to left by 0.0002 seconds on the time axis to account for an apparent time difference between the experiment and the analytical solution. The experimental-analytical correlation at an early time (peak strain prediction) was found to be good, and also for the dominant response frequency of the geocontainer. The predicted strains oscillation for longer times suggest that modeling of hydrodynamic drag damping and viscous losses by applying mass damping to geocontainer could be improved. The history plots for the axially directed strains at location C_1 were also drawn. The initial peak response (high frequency) obtained from analysis was not observed in the experimental data. This may be due to the sampling rate and filtering techniques used to obtain the data or to high strains being averaged over the effective length of the strain gauge. Excluding this trend, the analytical solution closely tracks the experimental data and provides conservative estimates for the peak response. The same trend was observed for history plots for the hoop directed strains at location A_2. The trends observed indicate that the overall analytical model provides a conservative estimate of cylinder's peak response and is therefore, appropriate for meeting the analysis objective.

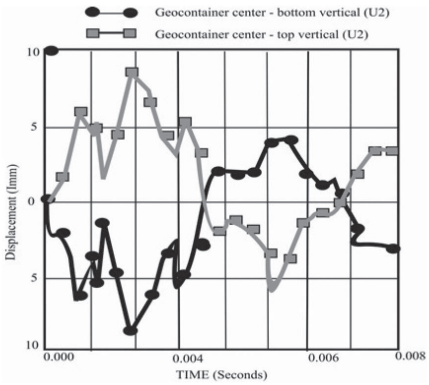

Figure 3. Displacement at the center of the endcaps of geocontainer.

8 CONCLUSIONS

The observations made establish fairly good correlations between experimental and analytical results and also the previously conducted experiments of similar nature though applicable to very different material and applications. This would be very helpful in dynamical designing of geocontainer systems and prediction of its behaviour under shock wave loadings. The geosynthetic material could be selected after taking into consideration the additional stresses and fatigue strains generated due to shock loadings. Further dynamical designing could incorporate restoring forces due to strapping or anchoring systems, variations of different fill materials and reliability analysis for design life of structure.

REFERENCES

Abaqus 6.5.1 (2005). "Finite element software," Abaqus/explicit, Abaqus Inc., USA.

Blevins, R.D. (1979). "Formulae for Natural Frequencies and Mode Shapes". Rober E. Forger Publishing Co.

Cotton, S.A. and Plaut, Plaut, R.A. (2003). "Two-dimen sional vibrations of Inflated geosynthetic tubes resting on rigid//deformable foundation". Blackburg, Virginia.

Huong, T.C. (2001). "Two-dimensional analysis of water-filled Geomembrane Tubes used as temporary flood-fighting devices", *M. S. Thesis*, Virginia Tech, Blacksburg, VA.

Klusman, C.R. (1998). "Two-Dimensional Analysis of Stacked Geosynthetic Tubes", M. S. Thesis, Virginia Tech, Blacksburg, VA.

Kim, M. (2003). "Two-Dimensional Analysis of Different Types of Water-filled Geomembrane Tubes as Temporary Flood-Fighting Devices, Ph.D. Dissertation, Virginia Tech, Blacksburg, VA.

Kwon and Fox (1993). "Underwater Shock Response of a Cylinder Subjected to a Side-on Explosion", Computers and Structures, Vol. 48, No. 4.

Plaut, R.H. and Klusman, C.R. (1999). "Two-dimensional analysis of stacked geosynthetic tubes on deformable foundations," *Thin-Walled Structures*, Vol. 34, pp. 179-194.

Plaut, R.H. and Suherman, S. (1998). "Two-dimensional analysis of geosynthetic tubes," *Acta Mechanica*, Vol. 129, pp. 207-218.